

# Analytical Methods

Accepted Manuscript



This is an *Accepted Manuscript*, which has been through the Royal Society of Chemistry peer review process and has been accepted for publication.

*Accepted Manuscripts* are published online shortly after acceptance, before technical editing, formatting and proof reading. Using this free service, authors can make their results available to the community, in citable form, before we publish the edited article. We will replace this *Accepted Manuscript* with the edited and formatted *Advance Article* as soon as it is available.

You can find more information about *Accepted Manuscripts* in the [Information for Authors](#).

Please note that technical editing may introduce minor changes to the text and/or graphics, which may alter content. The journal's standard [Terms & Conditions](#) and the [Ethical guidelines](#) still apply. In no event shall the Royal Society of Chemistry be held responsible for any errors or omissions in this *Accepted Manuscript* or any consequences arising from the use of any information it contains.

Cite this: DOI: 10.1039/c0xx00000x

www.rsc.org/xxxxxx

ARTICLE TYPE

## Fast protein detection from raw blood by size-exclusion SPR sensing

Kyohei Terao,<sup>\*a,b</sup> Shin-ichi Hiramatsu,<sup>a</sup> Takaaki Suzuki,<sup>a</sup> Hidekuni Takao,<sup>a</sup> Fusao Shimokawa<sup>a</sup>,  
Fumikazu Oohira<sup>a</sup>

Received (in XXX, XXX) Xth XXXXXXXXXX 20XX, Accepted Xth XXXXXXXXXX 20XX

DOI: 10.1039/b000000x

We developed a simple technique for detecting protein in raw blood samples using size-exclusion surface plasmon resonance (SPR) sensing. We designed a sensor chip consisting of a microslit array fabricated on a flat gold surface with gaps that were smaller in size than a mammalian red blood cell, which was designed for use in various Kretschmann-type SPR instruments. Blood cells were blocked by the microwalls, whereas the serum reached the SPR sensing field, enabling cell filtration and immediate protein detection in a one-step operation that required only the dispensing of a blood sample onto the chip. We evaluated the influence of the chip structure on SPR characteristics, and demonstrate using a whole blood sample from horse that IgG can be detected by the chip within 100 s of application.

### Introduction

Whole blood testing is widely performed for early detection of diseases by measuring specific biomarker proteins in blood serum<sup>1</sup>. Conventional methods involve time-consuming procedures and specialized equipment to separate blood cells from raw blood, such as a centrifuge or filtration devices that preclude the miniaturization of the system<sup>2, 3</sup>. Although various cell separation techniques have been developed to overcome these drawbacks – including those based on microfluidic and electrostatic cell separation<sup>2, 4, 5</sup> – most still require external devices such as pumps, tubes, valves, and power supplies. In addition, the integration of the separation and detection steps on a single chip remains a technical challenge.

To address these points, we developed a simple method of protein detection from a small volume of raw blood based on size-exclusion surface plasmon resonance (SPR) sensing<sup>6</sup>. This approach combines on-chip particle separation with the detection of changes in refractive index on the sensor surface via measurement of SPR angle. SPR has an advantage over other sensing methods in terms of rapidity and ease of operation because it does not require sample labelling<sup>3, 7–12</sup>; analytes are detected simply by applying the sample solution onto the ligand-immobilised sensor chip and measuring the shift in SPR angle caused by the specific binding of the analyte to the sensor surface. SPR measurement systems are widely used for research purposes, with most commercially available systems employing a Kretschmann-type configuration<sup>8, 13, 14</sup> (e.g., Biacore<sup>15</sup>). Recently, desktop- and the palm-top size systems have been commercialized and are expected to broaden the application of the SPR system to use in the field, such as for point-of-care testing<sup>14</sup>.

We developed an SPR chip for use in Kretschmann-type SPR systems. The chip has a microslit array fabricated on a flat gold

surface, with gaps smaller than the size of a mammalian red blood cell (RBC) (Fig. 1a). It is henceforth referred to as a filter chip to distinguish it from the standard flat chip sensor that has a flat gold surface. The SPR signal is associated with changes in refractive index in the field 300 nm above the gold surface. The microwalls of the filter chip exclude blood cells from this sensing field and allow only the serum to contact the sensor surface where ligands are immobilised to capture analytes; this allows the detection of specific proteins, which is reflected as a shift in SPR angle. This method does not require separate equipment for cell filtration since it is driven by sedimentation and diffusion – that is, cell filtration and detection are fully integrated on a single chip with the microwall structures – nor additional components to be installed in SPR instruments. Furthermore, the short distance between filtration and sensing fields – defined by microwall height – enables the detection of proteins immediately after sample application.

We first describe how the filter chip was designed to exclude RBCs and evaluate the influence of the microwall structure on SPR characteristics. We demonstrate using a raw blood that filtration and detection can be achieved within 100 s of sample application.

### Design and Simulation

#### Chip design

A particle with a diameter smaller than the slit gap ( $d_f$ ) can enter the slit and reach the sensing field in the same manner as for a conventional flat chip. If the particle is larger than  $d_f$  it remains separated from the chip surface by steric hindrance from the microwalls (Fig. 1 a, b). We designed the slit array such that RBCs would be excluded. An RBC has an oval-disk shape and is approximately 3  $\mu\text{m}$  thick. Considering the size and yield of the microwall, a gap size ( $d_f$ ) of 3  $\mu\text{m}$  was chosen. The walls were straight with a height,  $h$ , of 5  $\mu\text{m}$  and the width,  $d_w$ , of 3  $\mu\text{m}$ . The

range of the sensing field,  $s$ , was intrinsically determined by the optical system of the SPR instrument<sup>16</sup>, and was approximately 200 nm in our setup. Thus, the walls had sufficient height to exclude RBCs from the sensing field.

Two sets of microslit array were fabricated on a flat gold chip that corresponded to detection and reference channels (Ch1 and Ch2, respectively, in Fig. 1c). Each array had an area of  $2 \times 8$  mm. The sensing area was located at the centre of the chip and was  $2 \times$

10 mm. The chip was placed on the SPR instrument so that the 10 arrays were oriented perpendicularly to the sensing area. This configuration ensured that the microwalls were parallel to the light path, securing the propagation of surface plasmon polaritons (SPPs) on the gold surface between the walls<sup>6</sup>. For the SPR measurement of blood samples, two polydimethylsiloxane (PDMS) wells were formed for Ch1 and Ch2.

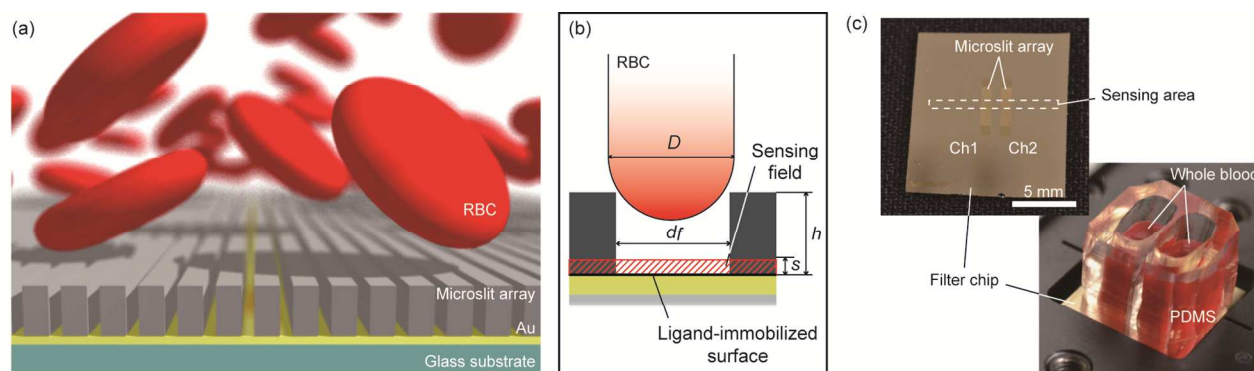


**Figure 1.** Size exclusion surface plasmon resonance (SPR) sensing for detecting proteins in whole blood. (a) Schematic illustration of the separation of red blood cells (RBCs) by a microslit array fabricated on a gold (Au) surface. (b) Dimensions of the microstructure. (c) Filter chip with two channels (Ch1, detection; Ch2, reference) and setup for SPR measurements of whole blood.

### SPR curve simulation

We estimated the effect of the filter chip microwalls on SPR characteristics. Although the microwalls were fabricated with photoresist SU-8, the light path was parallel to the flat sensor surface between the walls, allowing the generation of evanescent waves and SPPs without scattering, as described in our previous report<sup>6</sup> (Fig. 2a).

The SPR angle is the angle of incident light at which reflectivity is at a minimum, and is dependent on the refractive index in the sensing field. The reflectivity curve associated with incident angle is referred to as the SPR curve. For the purpose of a simple estimation, the effect of the interface between the walls and sensor surface was disregarded. In Kretschmann-type SPR measurement systems, reflectivity is determined by the intensity ratio of reflected to incident light. Given that reflected light intensity ( $I'$ ) is the sum of the intensities of light reflected from the sensor and walls, the reflectivity of the filter chip,  $R_{filter}$  ( $= I' / I$ ), depends on the ratio of their surface areas, which is described

$$R_{filter} = \frac{d_w}{d_w + d_f} R_w + \frac{d_f}{d_w + d_f} R_s \quad (1)$$

where  $R_s$ ,  $R_w$ ,  $d_w$ , and  $d_f$  are the reflectivities of the sensor and wall areas and the gap and width of the wall, respectively. These were simulated with Winspall software, which was used to calculate  $R_{filter}$  with equation 1 (Fig. 2b). We used 1.67 and 1.33 as the refractive indices of the photoresist (SU-8) and buffer solution, respectively. The  $R_w$  curve was constant in the range of SPR measurement angles (black line in Fig. 2b), whereas  $R_s$  had the same curve as for the flat chip, with a large depression at the SPR angle.

When the ratio of gold ( $d_f$ ) increased from 0:1 to 1:0 ( $d_f : d_w$ ), the intensity at the SPR angle gradually increased until it reached that of the flat chip. A filter chip has the same SPR angle as a flat chip, although the large area of the surface SU-8 wall introduces an uncertainty in the determination of SPR angles due to the small depression at the SPR angle<sup>17, 18</sup>. We therefore evaluated the effect of the ratio experimentally and compared it with the results obtained from this model.

Cite this: DOI: 10.1039/c0xx00000x

www.rsc.org/xxxxxx

ARTICLE TYPE

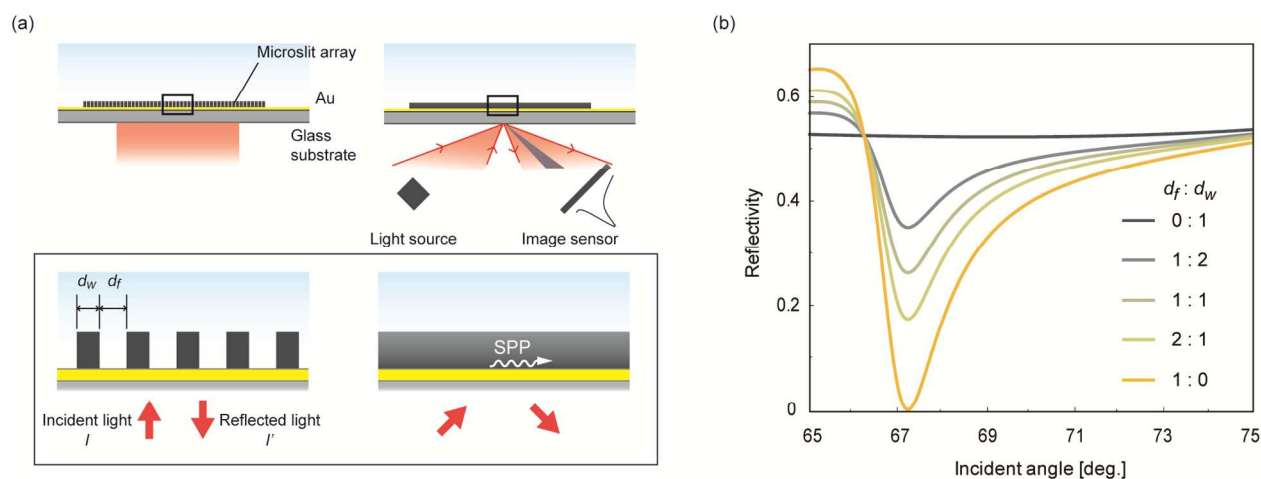


**Figure 2.** Theoretical estimation of the surface plasmon resonance (SPR) curve of the filter chip. (a) Configuration of the filter chip in SPR sensing. The inset shows an enlarged image of the microslit array. SU-8 walls were aligned parallel to the light path to allow surface plasmon polariton (SPP) propagation between them. (b) SPR curves of filter chips with different  $d_f : d_w$  (Au : SU-8) ratios of surface area.

## 5 Materials and Methods

### Fabrication

Glass chips (BK7, refractive index 1.515,  $16 \times 16 \times 1$  mm; NTT-AT Corp., San Jose, CA, USA) were cleaned with a piranha solution ( $\text{H}_2\text{SO}_4:\text{H}_2\text{O}_2 = 3:1$ ) for 10 min at  $85^\circ\text{C}$  and washed three times with pure water. Titanium was deposited to a 5-nm thickness as an adhesive layer followed by a 45-nm-thick gold layer using a thermal deposition system (VPC-1100; ULVAC Technologies, Inc., Methuen, MA, USA). Microwall structures of various  $d_f / d_w$  (Fig. 2a) were fabricated by standard UV-lithography of SU-8 3005 (MicroChem Corp., Newton, MA, USA).

### Chip verification

Surface structure was visualized by scanning electron microscopy (JFC-1600; JEOL Ltd., Tokyo, Japan). The sizes of three filter chips were measured. Height was measured with an optical profiler (NT-9100; Bruker AXS K.K., Yokohama, Japan). SPR curves of pure water were measured on both filter and flat chips using a Kretschmann-type SPR instrument with multi-detection channels (Smart SPR; NTT-AT Corp.) and an incident angle ranging from  $65^\circ$  to  $75^\circ$  and a 770-nm wavelength light source. For SPR measurements, a filter chip was placed on the glass prism such that the beam fit inside the area of the microslit array and slits were aligned parallel to the light path to minimize SPP scattering. A 100- $\mu\text{l}$  volume of pure water was dispensed into the well formed by a PDMS block with two holes in which SPR curves were measured. SPR angles of the filter and flat chips were monitored. Sensor chips were also characterized by measuring 15% sucrose solution.

## 35 SPR-based immunoassay for IgG detection

Anti-rabbit IgG antibody (goat polyclonal; Sigma-Aldrich Co., St. Louis, MO, USA) was covalently immobilised on the sensor surface at Ch1 as follows. All the operation for applying solution to the chip was performed manually in a PDMS well in this paper (batch-type experiment). Sensor chips were treated with UV-ozone cleaner (UV253H; Filgen, Inc., Tokyo, Japan) prior to surface modification. A carboxy-terminated self assembled monolayer (SAM) was formed on the gold surface of the sensor chip by incubation for 12 h in a solution of 10 nM 4,4'-dithiodibutyric acid in phosphate-buffered saline (PBS). A solution of 0.1 M 1-ethyl-3(3-dimethylaminopropyl) carbodiimide hydrochloride (EDC) and 0.05 M N-hydroxysuccinimide (NHS) in PBS was dispensed onto the chip followed by incubation for 12 min to activate the carboxyl groups. The anti-IgG solution (50  $\mu\text{g}/\text{ml}$ ) was then applied, followed by a 12-min incubation to induce covalent immobilisation by cross linking the amino groups of IgG molecules and the carboxyl groups of the SAM layer. After applying 1 M ethanolamine in PBS to block nonspecific adsorption and deactivate unreacted NHS ester groups on the surface, 0.50  $\mu\text{g}$ –5.0 mg/ml IgG (rabbit; Sigma-Aldrich Co.) in PBS was dispensed onto the chip and the SPR angle shift was monitored. As a reference, the same procedure was also performed for Ch2 to have anti-bovine serum albumin (BSA) antibodies on the sensor surface using 0.50 mg/ml anti-BSA antibody solution (sheep polyclonal; Bethyl Laboratories Inc., Montgomery, TX, USA). To exclude the effects of nonspecific binding to the sensor surface and thermal drift, we evaluated the signal obtained by subtracting the Ch2 SPR angle from that of Ch1. The detection channel (Ch1) has antibodies to capture IgG molecules specifically in a sample solution, whereas the reference channel (Ch2) having anti-BSA

antibody surface brings no specific binding of IgG and thus only a nonspecific adsorption occurs. Assuming that the detection channel has the same amount of non-specific adsorption as that of the reference channel, the subtraction gives the signal of IgG binding. To simplify the measurements, we employed this compensation for removing nonspecific adsorption.

### Detection of IgG in raw blood

Whole horse blood (Nippon Biotest Laboratories Inc., Tokyo, Japan) was used as a test sample. To evaluate cell filtration capacity, signals from both flat and filter chips were measured. Once the SPR angle had stabilized, the whole blood sample was added to the PDMS wells and the change in angle was monitored for 10 min.

To determine whether protein could be detected in raw blood, whole horse blood containing IgG molecules (from 5.0  $\mu\text{g/ml}$  to 5.0  $\text{mg/ml}$ ) was applied to the ligand-immobilised sensor chip and the presence of IgG was detected as an SPR angle shift.

## Results and Discussion

### Chip verification

SU-8 microwalls separated by gaps were fabricated on a gold surface (Table 1 and Fig. 3a). The height of the walls was  $5.7 \pm 0.5 \mu\text{m}$  (mean  $\pm$  SD,  $n = 5$ ).

SPR curves for pure water and 15% sucrose solution were generated from filter chips of various surface area ratios (Fig. 3b).

Our previous study showed that the filter chip has an SPR curve similar to that of the flat chip. The SPR angle was used to determine the change in refractive index within the sensing area. The depression at the SPR angle ( $n = 4$ ; Table 1) increased with decreases in the wall area, as predicted from our calculations; these along with equation 1 indicated that the normalized depression had the same value as the surface area ratio. The discrepancy between the experimental data and calculated value may have been due to measurement errors in the SEM analysis: although the width of the top of the wall was measured, the width

of the bottom dictates the depression at the SPR angle. The curve for 15% sucrose solution indicated that the filter chip had the same SPR angle shift as the flat chip.

The chip with a ratio of 1:2 ( $d_f : d_w$ ) showed the smallest depression at the SPR angle, suggesting an unstable time course for or failure to determine the angle using our experimental setup. We therefore used chips with a 1:1 or 2:1 ratio for protein detection in subsequent experiments.

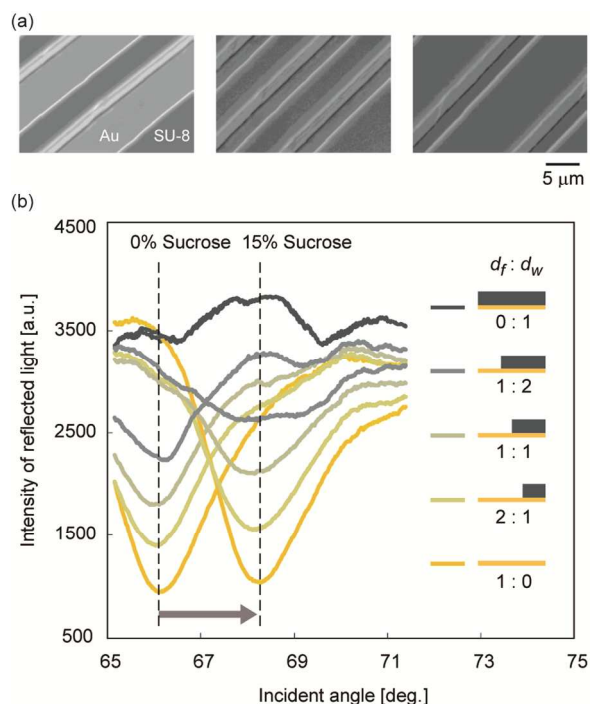


**Figure 3.** Experimental evaluation of filter chips with different  $d_f : d_w$  (Au : SU-8) ratios of surface area. (a) Scanning electron micrographs of filter chips; 2:1, 1:1, 1:2 (Au:SU-8). (b) Surface plasmon resonance curves of pure water and 15% sucrose solution measured with filter chips, SU-8-covered chip, and a bare gold (flat) chip.

**Table 1.** Relationship between area of the Au surface and depression in intensity at the SPR angle

Width [ $\mu\text{m}$ ]: Au/SU-8 (design)	Width [ $\mu\text{m}$ ]: Au/SU-8 (measured value)	Light intensity at the SPR angle (mean $\pm$ S.D.) [a.u.]	Surface area ratio (Au/total area)	Normalized depression at the SPR angle
covered with SU-8	- / -	$3499.1 \pm 60.3$	0.00	0.00
4 / 8	4.52 / 7.29	$2572.0 \pm 121.7$	0.26	0.40
4 / 4	4.41 / 3.26	$2182.5 \pm 144.8$	0.42	0.58
8 / 4	8.52 / 3.02	$1763.7 \pm 106.7$	0.61	0.76
Bare Au	- / -	$1237.2 \pm 42.2$	1.00	1.00

### Immunoassay on a filter chip

We tested the immunoassay on a filter chip using IgG as a model protein. To evaluate the sensor characteristics, we detected IgG in PBS ( $n = 4$ ; Fig. 4). The results show that the signal increased with protein concentration, suggesting that the filter chip can effectively detect proteins in solution. There was no signal detected at a protein concentration of 0.50  $\mu\text{g/ml}$  with either chip using our setup.

The effect of the microwalls on the diffusion of IgG molecules

was estimated. The time for diffusion across the typical distance can be calculated by  $T = L^2/2D$ , where  $L$  corresponds to the height of the wall ( $5.7 \mu\text{m}$ ) and  $D$  is the diffusion coefficient of a IgG molecule which is  $\approx 4.4 \times 10^{-11} \text{ m}^2/\text{s}$ <sup>19</sup>. The diffusion time is estimated to be 0.37 s, showing that it is fast compared to the time for reaching the equilibrium of binding ( $\sim 100$  s). Thus, IgG molecules rapidly fill the space between the microwalls and the detection should be comparable to that with the conventional flat chip.

The kinetic constants were estimated from the results, as follows.

The binding to the sensor surface is expressed as,

$$\frac{dr}{dt} = k_{on}C(r_{max} - r) - k_{off}r \quad (2)$$

where  $r$ ,  $r_{max}$ ,  $k_{on}$ ,  $k_{off}$ ,  $C$  are the response to the binding of analyte at a given time, the maximum response, the association and dissociation rate constant, and the concentration of the analyte on the surface, respectively<sup>20</sup>. At equilibrium,  $dr/dt$  is zero, and thus:

$$r_{eq} = \frac{Cr_{max}}{C + K_D} \quad (3)$$

where  $r_{eq}$  and  $K_D = k_{off} / k_{on}$  are the SPR response at equilibrium and the dissociation constant, respectively. From the curve fitting of (3) to the responses showed in Fig. 4, the  $K_D$  values were obtained;  $2.9 \times 10^{-7}$  M (flat chip) and  $6.7 \times 10^{-7}$  M (filter chip). These are comparable to the value reported in the literature ( $6.2 \times 10^{-7}$  M)<sup>20</sup>.

Although the SPR angle shifts of the filter and flat chips showed similar curves, the signal decreased slightly in the concentration range of 5.0–50  $\mu\text{g/ml}$ . This may be attributed to the fact that liquid replacement between the walls was prevented in the process of antibody immobilisation. The filter chip is intended for one sample use. The high reproducibility of the ligand immobilization is a key factor for protein analysis. The use of flow cell and the automated operation in the preparation step would be the solution to this problem. Although this limited the detection of low concentrations of protein, the ease of operation still offers an advantage in various applications of this chip.

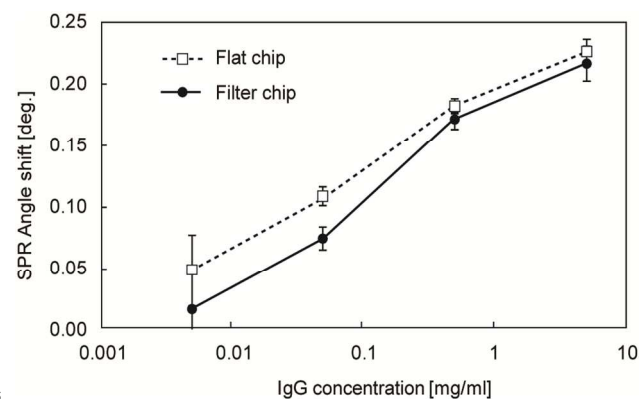


**Figure 4.** Detection of IgG molecules in PBS using flat and filter chips.

#### Detection of blood IgG

We measured IgG in whole horse blood at concentrations ranging from 5.0  $\mu\text{g}$ –50  $\text{mg/ml}$  (Fig. 5) without sample dilution. The time course of the SPR angle shows an increase following application of the sample to both filter and flat chips (Fig. 5a). For the latter, the signal continuously increased and we were therefore unable to determine the signal associated with protein binding. This may have been caused by the gradual sedimentation of blood cells that accumulated in the SPR sensing field. In contrast, the signal for the filter chip reached a plateau within 100 s of sample application, indicating that settling cells were successfully

excluded. These results demonstrate that the filter chip can separate blood cells from a raw blood sample simply by dispensing the sample onto the chip. Although the signal was slightly lower than in PBS, IgG was detected in whole horse blood ( $K_D = 7.5 \times 10^{-7}$  M, Fig. 5b), suggesting that our chip can be used as a rapid and simple method for testing blood from a raw sample.

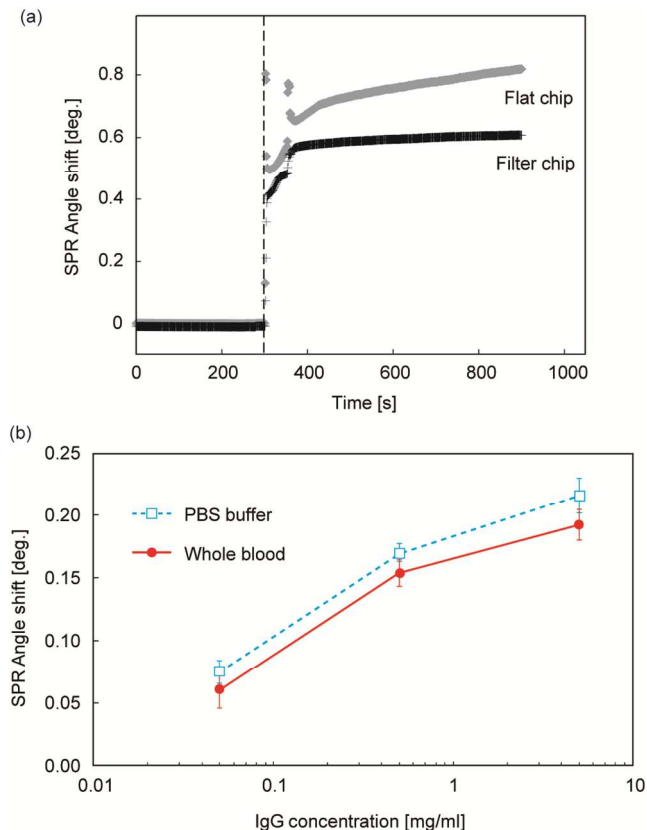


**Figure 5.** Detection of IgG in a whole horse blood sample without dilution. (a) Comparison of SPR sensorgrams between whole blood sample applied to filter and flat chips. The broken line shows the timing of blood application. (b) Detection of IgG in PBS and in whole blood using the filter chip.

#### Conclusions

We developed a simple blood testing method based on an SPR sensor chip with an integrated cell filtration function. The microslit array was fabricated with standard SU-8 photolithography. We evaluated the SPR sensing characteristics of chips with various SU-8 areas using pure water and sucrose solutions. The chip showed a sensing performance similar to conventional sensor chips with comparable dependence of the sensing curve on the area (width) of the SU-8, supporting our simple SPR model. We confirmed the cell filtration effect and demonstrated that SPR sensing of proteins from a raw blood sample can be achieved within 100 s. For realizing a point of care testing, it still requires the optimization of ligand immobilization and the high sensitivity for detecting low-concentration proteins, though, this filter chip technique will bring the opportunity to make a whole blood testing fast and simple.

## Acknowledgements

This work was partly supported by a Japan Society for the Promotion of Science KAKENHI (grant numbers 25630095 and 23710145) from the Ministry of the Education, Culture, Sports, Science and Technology (MEXT), and a research grant from the Asahi Glass Foundation. The work was carried out in part at the Kagawa University Nano-Processing Facility and supported by the Nanotechnology Platform Program of the MEXT.

## Notes and references

- <sup>10</sup> <sup>a</sup>Department of Intelligent Mechanical Systems Engineering, Kagawa University, 2217-20 Hayashi-cho, Takamatsu 761-0396, Japan. Fax: 81-87-864-2346; Tel: 81-87-864-2346; E-mail: terao@eng.kagawa-u.ac.jp
- <sup>15</sup> <sup>b</sup>JST, PREST 4-1-8 Honcho, Kawaguchi, Saitama 332-0012, Japan.
- <sup>15</sup> <sup>†</sup>Electronic Supplementary Information (ESI) available: [details of any supplementary information available should be included here]. See DOI: 10.1039/b000000x/
1. H. Jiang, X. Weng and D. Li, *Microfluid. Nanofluid.*, 2011, 10, 941–964.
  2. M. Toner and D. Irimia, in *Annu. Rev. Biomed. Eng.*, 2005, pp. 77–103.
  3. L. Gervais, N. De Rooij and E. Delamarche, *Adv. Mater.*, 2011, 23, H151–H176.
  4. X. Chen, D. F. Cui, C. C. Liu and H. Li, *Sensors and Actuators B-Chemical*, 2008, 130, 216–221.
  5. Z. T. F. Yu, K. M. Aw Yong and J. Fu, *Small*, 2014, 10, 1687–1703.
  6. K. Terao, K. Shimizu, N. Miyanishi, S. Shimamoto, T. Suzuki, H. Takao and F. Oohira, *Analyst*, 2012, 137, 2192–2198.
  7. X. D. Hoa, A. G. Kirk and M. Tabrizian, *Biosens. Bioelectron.*, 2007, 23, 151–160.
  8. J. Homola, *Anal. Bioanal. Chem.*, 2003, 377, 528–539.
  9. J. Homola, *Chem. Rev.*, 2008, 108, 462–493.
  10. N. Nagase, K. Terao, N. Miyanishi, K. Tamai, N. Uchiyama, T. Suzuki, H. Takao, F. Shimokawa and F. Oohira, *Analyst*, 2012, 137, 5034–5040.
  11. J. Trevino, A. Calle, J. M. Rodriguez-Frade, M. Mellado and L. M. Lechuga, *Clin. Chim. Acta*, 2009, 403, 56–62.
  12. J. Homola, S. S. Yee and G. Gauglitz, *Sensors and Actuators B-Chemical*, 1999, 54, 3–15.
  13. K. Kurihara and K. Suzuki, *Anal. Chem.*, 2002, 74, 696–701.
  14. W. M. Mullett, E. P. C. Lai and J. M. Yeung, *Methods-a Companion to Methods in Enzymology*, 2000, 22, 77–91.
  15. M. Fivash, E. M. Towler and R. J. Fisher, *Curr. Opin. Biotechnol.*, 1998, 9, 97–101.
  16. W. Knoll, *Annu. Rev. Phys. Chem.*, 1998, 49, 569–638.
  17. P. M. Boltovets and B. A. Snopok, *Talanta*, 2009, 80, 466–472.
  18. J. M. Rooney and E. A. H. Hall, *Anal. Chem.*, 2004, 76, 6861–6870.
  19. B. Pokric and Z. Pucar, *Anal. Biochem.*, 1979, 93, 103–114.
  20. Y. Dong, et al., *Anal. Bioanal. Chem.*, 2008, 390, 1575–1583.